Journal of Hazardous Materials 176 (2010) 466–472

Contents lists available at ScienceDirect

Journal of Hazardous Materials

journal homepage: www.elsevier.com/locate/jhazmat

Predicting competitive adsorption behavior of major toxic anionic elements onto activated alumina: A speciation-based approach

Tingzhi Su[a,b], Xiaohong Guan[c], Yulin Tang[a,b], Guowei Gu[b], Jianmin Wang[a,*]

[a] Department of Civil, Architectural and Environmental Engineering, Missouri University of Science and Technology, 1870 Miner Circle, Rolla, MO 65401, USA
[b] College of Environmental Science and Engineering, Tongji University, Shanghai 200092, PR China
[c] School of Municipal and Environmental Engineering, Harbin Institute of Technology, Harbin 150001, PR China

ARTICLE INFO

Article history:
Received 5 August 2009
Received in revised form 5 October 2009
Accepted 6 November 2009
Available online 13 November 2009

Keywords:
Arsenic
Selenium
Vanadium
Activated alumina
Competitive adsorption
Speciation-based model

ABSTRACT

Toxic anionic elements such as arsenic, selenium, and vanadium often co-exist in groundwater. These elements may impact each other when adsorption methods are used to remove them. In this study, we investigated the competitive adsorption behavior of As(V), Se(IV), and V(V) onto activated alumina under different pH and surface loading conditions. Results indicated that these anionic elements interfered with each other during adsorption. A speciation-based model was developed to quantify the competitive adsorption behavior of these elements. This model could predict the adsorption data well over the pH range of 1.5–12 for various surface loading conditions, using the same set of adsorption constants obtained from single-sorbate systems. This model has great implications in accurately predicting the field capacity of activated alumina under various local water quality conditions when multiple competitive anionic elements are present.

1. Introduction

Arsenic, selenium, and vanadium in water are of great concern due to their toxicity and carcinogenicity [1–3]. Arsenic and selenium are regulated by the US Environmental Protection Agency (EPA) in primary drinking water standards, with maximum contaminant levels (MCLs) of 10 μg/L and 50 μg/L, respectively [4]. Vanadium has been consistently listed on the EPA Contaminant Candidate Lists, CCL 1–CCL 3 [5–7], and a notification level of 50 μg/L has been set by State of California for drinking water [8]. Activated alumina adsorption has been widely used to remove arsenic, selenium, and vanadium [9–12]. Many researchers have reported that anions such as selenium, vanadium, phosphate, sulfate, and silicic could significantly reduce arsenic adsorption by various adsorbents [13–17]. Because co-existing anions may compete with each other, an accurate prediction of the competitive adsorption performance among these anions, under different water quality conditions especially pH and anion concentrations, is important in determining the field capacity of an adsorption media.

Models have previously been developed to predict the adsorption behavior of some toxic anions. These models include the constant capacitance model [16,18], the diffuse layer model [19], the triple layer model [20], the basic Stern model [20], the generalized two-layer model [17], and the CD-MUSIC model [13,21]. These models are generally very complex due to the inclusion of the surface electrostatic effect. Some of these models require several sets of adsorption constants with each set only applicable for a specific pH range and/or surface loading range. These drawbacks have severely limited the application of these models for predicting the sorbent capacity under different water quality conditions in the field.

Arsenic, selenium, and vanadium are commonly found in the forms of As(III) and As(V), Se(IV) and Se(VI), V(IV) and V(V) in aquatic systems [22–24]. Adsorption of their environmentally stable forms, As(V), Se(IV), and V(V) onto activated alumina in single element systems was investigated in our recent study [12]. We found that pH and surface loading were important for adsorption of these elements. However, the electrostatic effect did not impact the adsorption of these elements. Therefore, a more straight-forward speciation-based model, which did not include the electrostatic effect, was developed to quantify the adsorption behavior of As(V), Se(IV), and V(V) in single-sorbate systems [12]. This model includes only three adsorption constants for each element, with each constant correlating to one adsorbable species of that element. This speciation-based model could simulate the adsorption of these elements very well over a wide pH range (pH 2–12), and under different surface loading conditions. It could also predict the adsorption performance under conditions that were not used for obtaining the adsorption constants. However, the performance of this model for multiple-sorbate systems, which are more complex

* Corresponding author. Tel.: +1 573 341 7503; fax: +1 573 341 4729.
E-mail address: wangjia@mst.edu (J. Wang).

0304-3894/$ – see front matter © 2009 Elsevier B.V. All rights reserved.
doi:10.1016/j.jhazmat.2009.11.052

but more commonly seen in the field, has not been validated. The objectives of this study were (i) to evaluate the competitive adsorption behavior among As(V), Se(IV), and V(V), under different pH and surface loading conditions; and (ii) to develop a speciation-based competitive adsorption model to predict the adsorption behavior in multiple-sorbate systems as effects of pH and surface loading, using only one set of adsorption constants.

2. Experimental

2.1. Chemicals, reagents, and analytical methods

Activated alumina used in this study was purchased from Tramfloc, Inc., Tempe, AZ. It has a BET area of 363 m^2/g. Reagent grade chemicals, Millipore de-ionized water (DI water), and trace metal grade nitric acid were used to prepare all solutions used in this study. Individual 10,000 mg/L stock solutions of As(V), Se(IV), and V(V) were each prepared in 2% HNO_3 using sodium hydrogen arsenate heptahydrate, sodium selenite, and sodium vanadate, respectively. Sodium nitrate of 0.01 M was employed as a background electrolyte.

An Orion pH meter (perpHecT LoR model 370) with an Orion pH electrode (model 9207BN) was used for pH measurements. Liquid samples generated in this study were filtered through 0.45-μm cellulose acetate filters, acidified, and analyzed using a PerkinElmer ICP-OES. The instrument detection limits for As, Se, and V were 0.07 mg/L, 0.08 mg/L, and 0.06 mg/L, respectively.

2.2. Batch adsorption experiments

Batch experiments were used to study the competitive adsorption of As(V), Se(IV), and V(V) as functions of pH and surface loading. For each series of 125 mL HDPE bottles, the initial concentration of the sorbent was fixed at 10 g/L, but the pH of different bottles was adjusted to different values covering a pH range of 1.5–12, using stock HNO_3 or NaOH solutions. All bottles were capped and shaken for 24 h after pH adjustment. The suspensions were filtered immediately after shaking was stopped. Filtrates were acidified and then analyzed using the PerkinElmer ICP-OES. The final pH values were measured and recorded as the equilibrium pH.

To study As(V) adsorption as effects of Se(IV) or V(V), the initial As(V) concentration was fixed at approximately 50 mg/L, and added concentrations of Se(IV) or V(V) ranged from 10 mg/L to 200 mg/L. The experiments for Se(IV) and V(V) adsorption, in the presence of other competing elements, were carried out in a similar way. In experiments dealing with competitive effects among all three elements, equivalent amounts (in mg/L) of As(V), Se(IV), and V(V) were mixed with concentrations that ranged from 10 mg/L to 200 mg/L.

A broad pH range, from 1.5 to 12, was selected to induce the protonation and deprotonation reactions of different types of surface sites. In practice, the arsenic content in residual sludges from arsenic removal systems ranged up to 10 mg/g [25,26]. Considering the presence of other competing anions in the system, the content of total adsorbed anionic elements is expected to be much greater. Therefore, a broad surface loading range, up to 60 mg/g in total sorbate amount, was used in this study. The experimental data in the broad surface loading range will help to reveal the maximum possible adsorption capacity of the media and the competitive adsorption behavior among different sorbates.

3. Results and discussion

3.1. Effect of pH and surface loading on As(V), Se(IV), and V(V) adsorption

As(V), Se(IV), and V(V) speciation in solution are pH dependent. H_3AsO_4, $H_2AsO_4^-$, $HAsO_4^{2-}$, and AsO_4^{3-} are the dominant

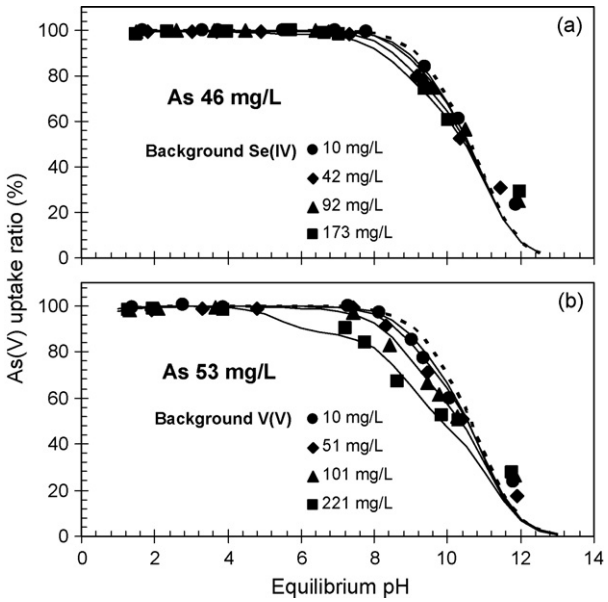

Fig. 1. As(V) adsorption in the presence of Se(IV) (a) or V(V) (b). Symbols are experimental data, solid lines are model predicted competitive adsorption results over pH 1.5–12.5, and dashed lines are model predicted results without competing anions. Experimental conditions: activated alumina = 10 g/L, temperature = 25 °C, equilibrium time = 24 h.

As(V) species in pH ranges of <2.26, 2.26–6.76, 6.76–11.29, and >11.29, respective. H_2SeO_3, $HSeO_3^-$, and SeO_3^{2-} are the dominant Se(IV) species in pH ranges of <2.62, 2.62–8.23, and >8.23, respectively. VO_2^+, H_3VO_4, $H_2VO_4^-$, HVO_4^{2-}, and VO_4^{3-} are the dominant V(V) species in pH ranges of <1.83, 1.83–3.4, 3.4–8.23, 8.23–13.5, and >13.5, respectively. Different elements species have different chemical properties. Therefore, adsorption of As(V), Se(IV), and V(V) onto activated alumina is pH dependent in single-sorbate systems [12].

Figs. 1–3 demonstrate the adsorption of As(V), Se(IV), and V(V) onto activated alumina in two-sorbate systems, respectively. Fig. 4 demonstrates the adsorption of these three elements in a three-sorbate system. Symbols in Figs. 1–4 are the experimental data over pH range of 1.5–12. Adsorption edges in these figures demonstrated that there was a maximum adsorption pH range for As(V), Se(IV), and V(V) in two-sorbate and three-sorbate systems, and beyond the pH range of the maximum adsorption, As(V), Se(IV), and V(V) adsorption could decrease substantially with the decrease (more acidic) or increase (more basic) of pH. The adsorption isotherms also indicated that the maximum adsorption range was narrowed down to a smaller pH range with the increase of total sorbate loading. For example, the pH range for the maximum adsorption in the three-sorbate system (Fig. 4) were 2–8, 2–5, 2–4, and approximately 3.5, for sorbate concentrations of approximately 10 mg/L, 50 mg/L, 100 mg/L, and 200 mg/L, respectively.

The effects of pH and surface loading on As(V), Se(IV), and V(V) adsorption observed in two-sorbate and three-sorbate systems are consistent with those in single-sorbate systems [12]. Our previous study indicated that the decrease of As(V), Se(IV), and V(V) adsorption over pH greater than maximum adsorption range was due to the fact that less protonated adsorption sites were available over pH > 8.8 [12]. Measurements of dissolved aluminum over the experimental pH range indicated that dissolution of activated alumina was negligible during the experiment (data not presented), thus the reduced adsorption of As(V), Se(IV), and V(V) at a pH less than 2 was not caused by the sorbent dissolution, suggesting that the neutral or positively charged species were not adsorbable onto an activated alumina surface.

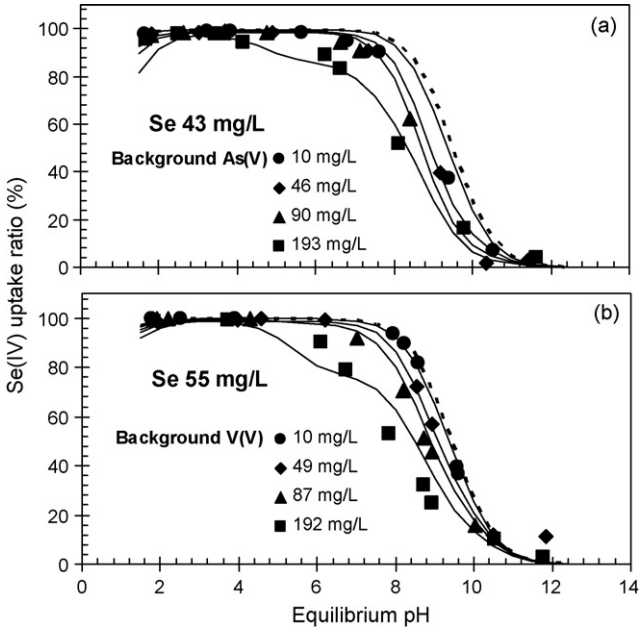

Fig. 2. Se(IV) adsorption in the presence of As(V) (a) or V(V) (b). Symbols are experimental data, solid lines are model predicted competitive adsorption results over pH 1.5–12.5, and dashed lines are model predicted adsorption results without competing anions. Experimental conditions: activated alumina = 10 g/L, temperature = 25 °C, equilibrium time = 24 h.

3.2. Competitive adsorption among As(V), Se(IV), and V(V) species

As shown in Figs. 1–3, when two elements co-existed in the system, the adsorption of one element decreased with the increase of the concentration of the other element. These data demonstrated the competitive adsorption among As(V), Se(IV), and V(V) onto activated alumina surface. The adsorption edges for two-sorbate systems in Figs. 1–3 indicated that competitive adsorption among

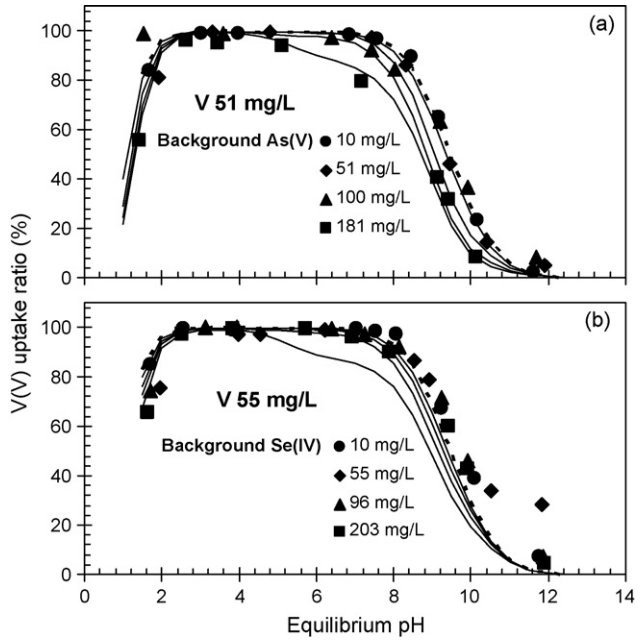

Fig. 3. V(V) adsorption in the presence of As(V) (a) and Se(IV) (b). Symbols are experimental data, solid lines are model predicted competitive adsorption results over pH 1–12.5, and dashed lines are model predicted results without competing anions. Experimental conditions: activated alumina = 10 g/L, temperature = 25 °C, equilibrium time = 24 h.

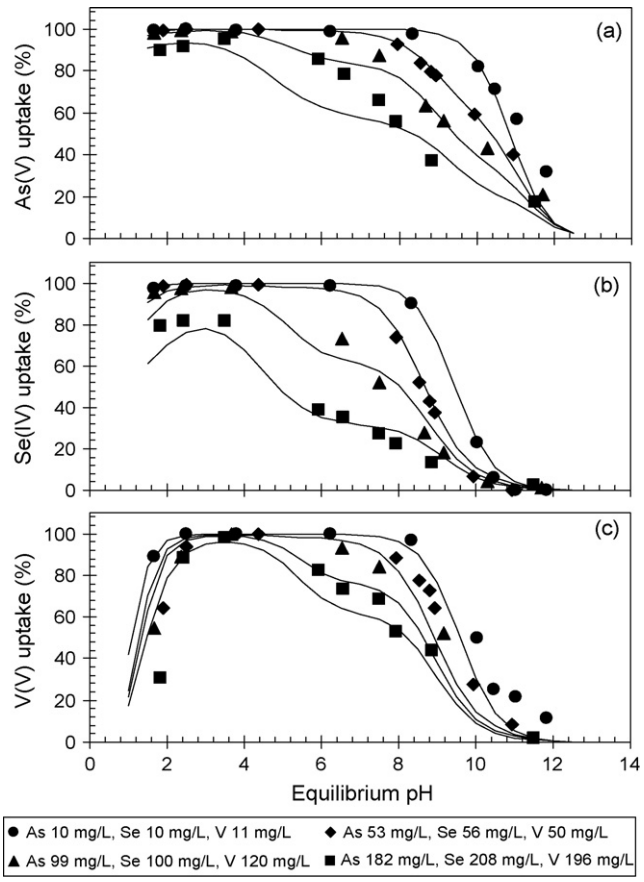

Fig. 4. As(V) (a), Se(IV) (b), and V(V) (c) adsorption results in three-sorbate systems. Symbols are experimental data, solid lines are model predicted competitive adsorption results over pH 1–12.5. Experimental conditions: activated alumina = 10 g/L, temperature = 25 °C, equilibrium time = 24 h.

As(V), Se(IV), and V(V) mainly occurred in the pH range of 7–10. This pH range could expand to pH range of 3.5–10.5 when the total surface loading increased to approximately 25 mg sorbate/g sorbent. In these pH ranges, $H_2AsO_4^-$, $HAsO_4^{2-}$, $HSeO_3^-$, SeO_3^{2-}, $H_2VO_4^-$, and HVO_4^{2-} were the dominant species. Therefore, competitive adsorption of As(V), Se(IV), and V(V) mainly occurred among these negatively charged species.

Dashed lines in Figs. 1–3 are predicted As(V), Se(IV), and V(V) adsorption data when competing elements do not exist. These predictions were made using the adsorption constants shown in Table 1, which were determined previously for single-sorbate systems [12]. Compared to the adsorption curve without competition (the dashed lines) in Fig. 1, 173 mg/L (2.2 mM) of Se(IV) and 101 mg/L (2 mM) of V(V), which are of similar molar concentration, resulted in almost the same degree of maximal reduction in As(V) adsorption at a pH range of 7–10. Therefore, Se(IV) and V(V) have similar adsorption affinity onto activated alumina surface. Similarly, comparing the experimental data points to the dashed curves in Fig. 2, by increasing the background As(V) to 193 mg/L (2.6 mM), or increasing the background V(V) to 192 mg/L (3.8 mM), the maximal reduction in Se(IV) adsorption was 30–40% and occurred in the pH range of 6–9 for both cases. In Fig. 3, 181 mg/L (2.4 mM) As(V) decreased V(V) adsorption maximally 25%, but 203 mg/L Se(IV) (2.6 mM) maximally decreased V(V) adsorption less than 10%. Based on the relative impact among these three elements, one can conclude that the adsorption affinities of these three elements on activated alumina surface sites followed an order of As(V) > V(V) > Se(IV), which is consistent with the adsorption constants shown in Table 1. This order is also in agreement with

Table 1
The density and acidity constant of activated alumina surface sites, and their adsorption constants for different As(V), Se(IV), and V(V) species [11].

Site	$\underline{S}_1$	$\underline{S}_{2W}$	$\underline{S}_{2S}$
Density (10^{-4} mol/g)	6.26	2.36	0.59
pK_H	3.33	6.57	
Adsorption constant			
As(V)	$\log K_{S1}^{As} = 3.9$ $\log K_{S2}^{As} = 5.1$	$\log K_{S4}^{As} = \log K_{S5}^{As} = \log K_{S6}^{As} = 5.1$	$\log K_{S7}^{As} = \log K_{S8}^{As} = \log K_{S9}^{As} = 7.6$
Se(IV)	$\log K_{S1}^{Se} = \log K_{S2}^{Se} = 3.3$	$\log K_{S4}^{Se} = \log K_{S5}^{Se} = 4.8$	$\log K_{S7}^{Se} = \log K_{S8}^{Se} = 6.3$
V(V)	$\log K_{S1}^{V} = 4.9$ $\log K_{S2}^{V} = 7.3$	$\log K_{S4}^{V} = \log K_{S5}^{V} = \log K_{S6}^{V} = 4.9$	$\log K_{S7}^{V} = \log K_{S8}^{V} = \log K_{S9}^{V} = 6.4$

Note: For As(V), K_{S1}^{As} and K_{S2}^{As} denote adsorption constants of $H_2AsO_4^-$ and $HAsO_4^{2-}$ to site $\underline{S}_1$, respectively; K_{S4}^{As}, K_{S5}^{As}, and K_{S6}^{As} denote adsorption constants of $H_2AsO_4^-$, $HAsO_4^{2-}$, and AsO_4^{3-} to site $\underline{S}_{2W}$, respectively; K_{S7}^{As}, K_{S8}^{As}, and K_{S9}^{As} denote adsorption constants of $H_2AsO_4^-$, $HAsO_4^{2-}$, and AsO_4^{3-} to site $\underline{S}_{2S}$, respectively. Similar assignments are used for Se(IV) and V(V). Superscripts in these expressions are used to differentiate the K_S values for As(V), Se(IV), and V(V), respectively. Adsorption of AsO_4^{3-} and are VO_4^{3-} onto site $\underline{S}_1$ are negligible and are not considered in the modeling.

other researchers' findings that As has a stronger affinity for adsorption on aluminum oxides and other sorbents than Se and V [15,27].

4. Modeling competitive adsorption of As(V), Se(IV), and V(V)

4.1. Background knowledge

To model the adsorption of As(V), Se(IV), and V(V) onto activated alumina in multi-sorbate systems, it is necessary to recap several of the findings in our previous study [12], which will be the base of the competitive adsorption model development in this study. In brief:

(a) Three types of monoprotic acidic sites on an activated alumina surface were assumed. They were $\underline{S}_1$, $\underline{S}_2$, and $\underline{S}_3$, respectively. Acid site $\underline{S}_2$ consisted of a weak adsorption site $\underline{S}_{2W}$ and a strong adsorption site $\underline{S}_{2S}$. Only the protonated fractions of sites $\underline{S}_1$, $\underline{S}_{2W}$, and $\underline{S}_{2S}$ were responsible for adsorbing anionic elements. Because they were positively charged, their deprotonation reactions can be expressed as:

$$\underline{S}_i OH_2^+ = \underline{S}_i OH + H^+ \quad K_{Hi} \tag{1}$$

where $\underline{S}_i = \underline{S}_1$, $\underline{S}_{2W}$, or $\underline{S}_{2S}$. K_{Hi} is the acidity constants of surface acid sites $\underline{S}_i$. Table 1 shows the density ($\underline{S}_{Ti}$) and acidity constant (K_{Hi}) of these adsorption sites.

(b) Only the negatively charged As(V), Se(IV), and V(V) species were adsorbable, and the electrostatic effect on their adsorption was negligible.

(c) Reactions of As(V), Se(IV), and V(V) with the surface sites of activated alumina followed 1:1 stoichiometry, and each site behaved independently, as if the other sites did not exist.

4.2. Models for As(V), Se(IV), and V(V) adsorption in two-sorbate systems

As aforementioned, adsorption of As(V), Se(IV), and V(V) onto activated alumina is surface reactions of the negatively charged As(V), Se(IV), and V(V) species with the protonated fractions of activated alumina surface sites $\underline{S}_1$, $\underline{S}_{2W}$ and $\underline{S}_{2S}$. These reactions are denoted in groups as Eq. (2), Eq. (3), and Eq. (4) for As(V), Se(IV), and V(V), respectively.

$$\begin{aligned} \underline{S}_i OH_2^+ + H_2AsO_4^- &= \underline{S}_i\text{–}H_2AsO_4 + H_2O \\ \underline{S}_i OH_2^+ + HAsO_4^{2-} &= \underline{S}_i\text{–}HAsO_4^- + H_2O \\ \underline{S}_i OH_2^+ + AsO_4^{3-} &= \underline{S}_i\text{–}AsO_4^{2-} + H_2O \end{aligned} \tag{2}$$

$$\begin{aligned} \underline{S}_i OH_2^+ + HSeO_3^- &= \underline{S}_i\text{–}HSeO_3 + H_2O \\ \underline{S}_i OH_2^+ + SeO_3^{2-} &= \underline{S}_i\text{–}SeO_3^- + H_2O \end{aligned} \tag{3}$$

$$\begin{aligned} \underline{S}_i OH_2^+ + H_2VO_4^- &= \underline{S}_i\text{–}H_2VO_4 + H_2O \\ \underline{S}_i OH_2^+ + HVO_4^{2-} &= \underline{S}_i\text{–}HVO_4^- + H_2O \\ \underline{S}_i OH_2^+ + VO_4^{3-} &= \underline{S}_i\text{–}VO_4^{2-} + H_2O \end{aligned} \tag{4}$$

The equilibrium constants of the above reactions are the adsorption constants (K_S) of different As(V), Se(IV), and V(V) onto each surface site. These adsorption constants have been modeled with the single-sorbate adsorption data in our former study [12] and listed in Table 1. The concentration of different acid sites $\underline{S}_i$ (i = 1, 2W, 2S), and different species of As(V), Se(IV), and V(V) in solution are expressed in Table 2.

In two-sorbate systems, such as a system containing As(V) and Se(IV), the surface reactions are Eqs. (2) and (3). The concentrations of adsorbed arsenic and selenium species onto site $\underline{S}_1$ are expressed using the following equations:

$$\begin{aligned} [\underline{S}_1\text{–}H_2AsO_4] &= K_{S1}^{As}\alpha_1^{As}[As(V)]_D[\underline{S}_1OH_2^+] \\ [\underline{S}_1\text{–}HAsO_4^-] &= K_{S2}^{As}\alpha_2^{As}[As(V)]_D[\underline{S}_1OH_2^+] \\ [\underline{S}_1\text{–}AsO_4^{2-}] &= K_{S3}^{As}\alpha_3^{As}[As(V)]_D[\underline{S}_1OH_2^+] \\ [\underline{S}_1\text{–}HSeO_3] &= K_{S1}^{Se}\alpha_1^{Se}[Se(IV)]_D[\underline{S}_1OH_2^+] \\ [\underline{S}_1\text{–}SeO_3^-] &= K_{S2}^{Se}\alpha_2^{Se}[Se(IV)]_D[\underline{S}_1OH_2^+] \end{aligned} \tag{5}$$

Because AsO_4^{3-} only exists in extremely basic pH conditions (pK_{a3} = 11.29), where surface site $\underline{S}_1$ (pK_{H1} = 3.33) is unavailable, the adsorbed AsO_4^{3-} species ($\underline{S}_1$–AsO_4^{2-}) is negligible. Therefore, the total site concentration $\underline{S}_{T1}$ is expressed as:

$$\begin{aligned} \underline{S}_{T1} &= [\underline{S}_1OH_2^+] + [\underline{S}_1OH] + [\underline{S}_1\text{–}H_2AsO_4] + [\underline{S}_1\text{–}HAsO_4^-] \\ &\quad + [\underline{S}_1\text{–}HSeO_3] + [\underline{S}_1\text{–}SeO_3^-] \end{aligned} \tag{6}$$

Base on Eq. (1):

$$[\underline{S}_1OH] = \frac{[\underline{S}_1OH_2^+]K_{H1}}{[H^+]} \tag{7}$$

Combining Eqs. (5)–(7), $[\underline{S}_1OH_2^+]$ can be expressed as:

$$[\underline{S}_1OH_2^+] = \frac{\underline{S}_{T1}\alpha_{1+}}{1 + \alpha_{1+}(\alpha_1^{As}K_{S1}^{As} + \alpha_2^{As}K_{S2}^{As})[As(V)]_D + \alpha_{1+}(\alpha_1^{Se}K_{S1}^{Se} + \alpha_2^{Se}K_{S2}^{Se})[Se(IV)]_D} \tag{8}$$

Table 2
Speciation calculation of surface sites $\underline{S}_i$, element As(V), Se(IV), and V(V) in solution.

Surface site speciation	$[\underline{S}_1OH_2^+] = \alpha_{1+}\underline{S}_{T1}$, $[\underline{S}_{2W}OH_2^+] = \alpha_{2+}\underline{S}_{T2W}$, $[\underline{S}_{2S}OH_2^+] = \alpha_{2+}\underline{S}_{T2S}$ $\alpha_{1+} = \frac{[H^+]}{[H^+]+K_{H1}}$, $\alpha_{2+} = \frac{[H^+]}{[H^+]+K_{H2}}$ $\underline{S}_{Ti}$ (i = 1, 2W, 2S) is the total concentration of $\underline{S}_i$ site; α_{1+} is the fraction of protonated site $\underline{S}_1$, α_{2+} is the fraction of protonated site $\underline{S}_{2W}$ and $\underline{S}_{2S}$; K_{H1} is the acidity constant of site $\underline{S}_1$, K_{H2} is the acidity constant of site $\underline{S}_{2W}$ and $\underline{S}_{2S}$.
As(V), Se(IV), and V(V) speciation	$[H_2AsO_4^-] = \alpha_1^{As}[As(V)]_D$, $[HAsO_4^{2-}] = \alpha_2^{As}[As(V)]_D$, $[AsO_4^{3-}] = \alpha_3^{As}[As(V)]_D$, $[HSeO_3^-] = \alpha_1^{Se}[Se(IV)]_D$, $[SeO_3^{2-}] = \alpha_2^{Se}[Se(IV)]_D$, $[H_2VO_4^-] = \alpha_1^{V}[V(V)]_D$, $[HVO_4^{2-}] = \alpha_2^{V}[V(V)]_D$, $[VO_4^{3-}] = \alpha_3^{V}[V(V)]_D$ α_1^{As}, α_2^{As}, and α_3^{As} are fractions of $H_2AsO_4^-$, $HAsO_4^{2-}$, and AsO_4^{3-} in solution. Similar arrangements are applied for Se(IV) and V(V). Superscripts in these expressions are used to differentiate the α values for As(V), Se(IV), and V(V), respectively. For As(V) and V(V): $\alpha_1 = \frac{[H^+]^2K_{a1}}{[H^+]^3+[H^+]^2K_{a1}+[H^+]K_{a1}K_{a2}+K_{a21}K_{a2}K_{a3}}$, $\alpha_2 = \frac{[H^+]K_{a1}K_{a2}}{[H^+]^3+[H^+]^2K_{a1}+[H^+]K_{a1}K_{a2}+K_{a1}K_{a2}K_{a3}}$, $\alpha_3 = \frac{K_{a1}K_{a2}K_{a3}}{[H^+]^3+[H^+]^2K_{a1}+[H^+]K_{a1}K_{a2}+K_{a1}K_{a2}K_{a3}}$ For Se(IV): $\alpha_1 = \frac{[H^+]K_{a1}}{[H^+]^2+[H^+]K_{a1}+K_{a1}K_{a2}}$, $\alpha_2 = \frac{K_{a1}K_{a2}}{[H^+]^2+[H^+]K_{a1}+K_{a1}K_{a2}}$ K_{a1}, K_{a2}, and K_{a3} are correspondent to the pK_a values of arsenate acid, selenite acid, or vanadate acid.

Therefore, the total adsorbed As(V) concentration on surface site $\underline{S}_1$ in the As(V)+Se(IV) system is expressed as:

$$[As(V)]_{ads} = \frac{\underline{S}_{T1}\alpha_{1+}(\alpha_1^{As}K_{S1}^{As}+\alpha_2^{As}K_{S2}^{As})[As(V)]_D}{1+\alpha_{1+}(\alpha_1^{As}K_{S1}^{As}+\alpha_2^{As}K_{S2}^{As})[As(V)]_D+\alpha_{1+}(\alpha_1^{Se}K_{S1}^{Se}+\alpha_2^{Se}K_{S2}^{Se})[Se(IV)]_D} \quad (9)$$

The total adsorbed As(V) concentration on surface site $\underline{S}_{2W}$ and $\underline{S}_{2S}$ can be generated similarly, and the total adsorbed As(V) on activated alumina is expressed as:

$$\begin{aligned}[As(V)]_{ads} = {} & \frac{\underline{S}_{T1}\alpha_{1+}(\alpha_1^{As}K_{S1}^{As}+\alpha_2^{As}K_{S2}^{As})[As(V)]_D}{1+\alpha_{1+}(\alpha_1^{As}K_{S1}^{As}+\alpha_2^{As}K_{S2}^{As})[As(V)]_D+\alpha_{1+}(\alpha_1^{Se}K_{S1}^{Se}+\alpha_2^{Se}K_{S2}^{Se})[Se(IV)]_D} \\ & + \frac{\underline{S}_{T2W}\alpha_{2+}(\alpha_1^{As}K_{S4}^{As}+\alpha_2^{As}K_{S5}^{As}+\alpha_3^{As}K_{S6}^{As})[As(V)]_D}{1+\alpha_{2+}(\alpha_1^{As}K_{S4}^{As}+\alpha_2^{As}K_{S5}^{As}+\alpha_3^{As}K_{S6}^{As})[As(V)]_D+\alpha_{2+}(\alpha_1^{Se}K_{S4}^{Se}+\alpha_2^{Se}K_{S5}^{Se})[Se(IV)]_D} \\ & + \frac{\underline{S}_{T2S}\alpha_{2+}(\alpha_1^{As}K_{S7}^{As}+\alpha_2^{As}K_{S8}^{As}+\alpha_3^{As}K_{S9}^{As})[As(V)]_D}{1+\alpha_{2+}(\alpha_1^{As}K_{S7}^{As}+\alpha_2^{As}K_{S8}^{As}+\alpha_3^{As}K_{S9}^{As})[As(V)]_D+\alpha_{2+}(\alpha_1^{Se}K_{S7}^{Se}+\alpha_2^{Se}K_{S8}^{Se})[Se(IV)]_D}\end{aligned} \quad (10)$$

Similarly, the As(V) adsorption model in the As(V) + V(V) system is derived, which is:

$$\begin{aligned}[As(V)]_{ads} = {} & \frac{\underline{S}_{T1}\alpha_{1+}(\alpha_1^{As}K_{S1}^{As}+\alpha_2^{As}K_{S2}^{As})[As(V)]_D}{1+\alpha_{1+}(\alpha_1^{As}K_{S1}^{As}+\alpha_2^{As}K_{S2}^{As})[As(V)]_D+\alpha_{1+}(\alpha_1^{V}K_{S1}^{V}+\alpha_2^{V}K_{S2}^{V})[V(V)]_D} \\ & + \frac{\underline{S}_{T2W}\alpha_{2+}(\alpha_1^{As}K_{S4}^{As}+\alpha_2^{As}K_{S5}^{As}+\alpha_3^{As}K_{S6}^{As})[As(V)]_D}{1+\alpha_{2+}(\alpha_1^{As}K_{S4}^{As}+\alpha_2^{As}K_{S5}^{As}+\alpha_3^{As}K_{S6}^{As})[As(V)]_D+\alpha_{2+}(\alpha_1^{V}K_{S4}^{V}+\alpha_2^{V}K_{S5}^{V}+\alpha_3^{V}K_{S6}^{V})[V(V)]_D} \\ & + \frac{\underline{S}_{T2S}\alpha_{2+}(\alpha_1^{As}K_{S7}^{As}+\alpha_2^{As}K_{S8}^{As}+\alpha_3^{As}K_{S9}^{As})[As(V)]_D}{1+\alpha_{2+}(\alpha_1^{As}K_{S7}^{As}+\alpha_2^{As}K_{S8}^{As}+\alpha_3^{As}K_{S9}^{As})[As(V)]_D+\alpha_{2+}(\alpha_1^{V}K_{S7}^{V}+\alpha_2^{V}K_{S8}^{V}+\alpha_3^{V}K_{S9}^{V})[V(V)]_D}\end{aligned} \quad (11)$$

Models of Se(IV) and V(V) adsorption in two-sorbate systems were developed similarly to that of As(V) above. They were included in Supplementary material, Eqs. (S1) and (S2) for Se(IV), and Eqs. (S3) and (S4) for V(V).

4.3. Models for As(V), Se(IV), and V(V) adsorption in three-sorbate systems

For three-sorbate systems where As(V), Se(IV), and V(V) coexist, the surface adsorption reactions are Eqs. (2)–(4). Models for As(V), Se(IV), or V(V) adsorption in three-sorbate systems were developed similarly as in Section 4.2. For example, the As(V) adsorption model is expressed as:

$$[\mathrm{As(V)}]_{ads} = \frac{\underline{S}_{T1}\alpha_{1+}(\alpha_1^{As}K_{S1}^{As} + \alpha_2^{As}K_{S2}^{As})[\mathrm{As(V)}]_D}{1 + \alpha_{1+}(\alpha_1^{As}K_{S1}^{As} + \alpha_2^{As}K_{S2}^{As})[\mathrm{As(V)}]_D + \alpha_{1+}(\alpha_1^{Se}K_{S1}^{Se} + \alpha_2^{Se}K_{S2}^{Se})[\mathrm{Se(IV)}]_D + \alpha_{1+}(\alpha_1^{V}K_{S1}^{V} + \alpha_2^{V}K_{S2}^{V})[\mathrm{V(V)}]_D} + \frac{\underline{S}_{T2W}\alpha_{2+}(\alpha_1^{As}K_{S4}^{As} + \alpha_2^{As}K_{S5}^{As} + \alpha_3^{As}K_{S6}^{As})[\mathrm{As(V)}]_D}{1 + \alpha_{2+}(\alpha_1^{As}K_{S4}^{As} + \alpha_2^{As}K_{S5}^{As} + \alpha_3^{As}K_{S6}^{As})[\mathrm{As(V)}]_D + \alpha_{2+}(\alpha_1^{Se}K_{S4}^{Se} + \alpha_2^{Se}K_{S5}^{Se})[\mathrm{Se(IV)}]_D + \alpha_{2+}(\alpha_1^{V}K_{S4}^{V} + \alpha_2^{V}K_{S5}^{V} + \alpha_3^{V}K_{S6}^{V})[\mathrm{V(V)}]_D} + \frac{\underline{S}_{T2S}\alpha_{2+}(\alpha_1^{As}K_{S7}^{As} + \alpha_2^{As}K_{S8}^{As} + \alpha_3^{As}K_{S9}^{As})[\mathrm{As(V)}]_D}{1 + \alpha_{2+}(\alpha_1^{As}K_{S7}^{As} + \alpha_2^{As}K_{S8}^{As} + \alpha_3^{As}K_{S9}^{As})[\mathrm{As(V)}]_D + \alpha_{2+}(\alpha_1^{Se}K_{S7}^{Se} + \alpha_2^{Se}K_{S8}^{Se})[\mathrm{Se(IV)}]_D + \alpha_{2+}(\alpha_1^{V}K_{S7}^{V} + \alpha_2^{V}K_{S8}^{V} + \alpha_3^{V}K_{S9}^{V})[\mathrm{V(V)}]_D} \quad (12)$$

Adsorption models for Se(IV) and V(V) in the As(V) + Se(IV) + V(V) system are similar in form, and are given in Supplementary material, Eqs. (S5) and (S6) respectively.

One may notice that the speciation-based model developed above for two-sorbate and three-sorbate systems are similar in form to the traditional Langmuir isotherm, however, they incorporate the pH effect, and the competition effect of different As(V), Se(IV), and V(V) species for the same adsorption site. Thus, the models developed in this study have the advantage over the traditional Langmuir isotherm when predicting the adsorption of As(V), Se(IV), and V(V) under different pH conditions and when other competing elements are present.

4.4. Modeling competitive adsorption of As(V), Se(IV), and V(V)

Speciation-based competitive models, Eqs. (10) and (11), (S1)–(S4), and the respective adsorption constants in Table 1, were used to predict adsorptions of As(V), Se(IV), and V(V) in two-sorbate systems. The solid lines in Figs. 1–3 are predicted results for As(V), Se(IV), and V(V), respectively, when the other two elements are present. The model prediction generally describes the experimental data very well over the entire experimental pH range and surface loading conditions. When the competing anion concentration was low (i.e., 10 mg/L), the competitive effect was not significant because the adsorption curve and the dotted lines (without competing ions) almost overlapped. However, when the competing anion concentration increased to greater than 50 mg/L, the competitive effect became obvious, especially in the pH range of 7–10.

Eqs. (12), (S5) and (S6) were used to predict competitive adsorption of As(V), Se(IV), and V(V) in three-sorbate systems, using the same set of adsorption constants in Table 1. Solid lines in Fig. 4 represent the predicted results and they are in good agreement with experimental data.

It should be noted that the values of all adsorption constants used in these models were generated independently using experimental data for single-sorbate systems [12], and the modeling results satisfactorily predict adsorption performance in multiple-sorbate systems. This study validated the speciation-based modeling approach for predicting the competitive adsorption behavior of activated alumina under various water quality conditions when competing elements are present.

4.5. Surface speciation of adsorbed As(V), Se(IV), and V(V) species

Fig. 5 shows the surface speciation profile of adsorbed As(V), Se(IV) and V(V) in the three-sorbate system, for initial concentrations of As(V) = 53 mg/L, Se(IV) = 56 mg/L, and V(V) = 50 mg/L. Surface speciation profiles for other initial concentrations in three-sorbate systems (10 mg/L each, 100 mg/L each, and 200 mg/L each, respectively) are shown in Supplementary material, Fig. S1–S3. Fig. 5 shows that As(V) was mostly adsorbed onto the strong $\underline{S}_2$ site, i.e. $\underline{S}_{2S}$. Se(IV) was mostly adsorbed onto the weak $\underline{S}_2$ site, i.e. $\underline{S}_{2W}$. V(V) was mostly adsorbed onto both the first acid site ($\underline{S}_1$) and the weak $\underline{S}_2$ site ($\underline{S}_{2W}$). The selectivity of these elements to these sites was determined by their respective adsorption constants. For example, Table 1 shows that site $\underline{S}_{2S}$ was the strongest adsorption site for all elements. It also had greater adsorption constants to As(V) species than to Se(IV) and V(V) species. Therefore, during the competitive adsorption, site $\underline{S}_{2S}$ first selected As(V) species. When site $\underline{S}_{2S}$ was fully occupied, other elements had to be adsorbed by other surface sites. Because site $\underline{S}_{2W}$ had a greater acidity constant (i.e. pK_H) than site $\underline{S}_1$ (Table 1), the protonated fraction of site $\underline{S}_{2W}$ was more readily available for adsorption than site $\underline{S}_1$. In addition, because site $\underline{S}_{2W}$ had similar adsorption constants toward both Se(IV) and V(V) species, it was responsible for adsorbing both

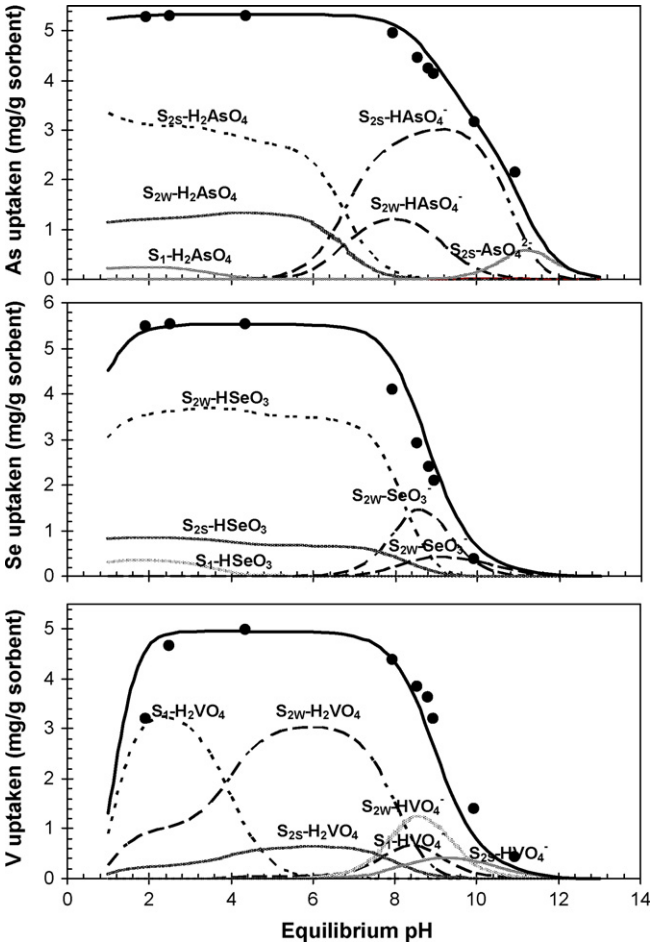

Fig. 5. Surface speciation profile of adsorbed As(V), Se(IV) and V(V) onto activated alumina in the three-sorbate system, for initial concentrations of As(V) = 53 mg/L, Se(IV) = 56 mg/L, and V(V) = 50 mg/L. Symbols are experimental data, solid lines are modeling results. Experimental conditions are same as Fig. 4.

Se(IV) and V(V), as indicated in Fig. 5. The rest of V(V) species were adsorbed by site $\underline{S}_1$ because $\underline{S}_1$ had a relative larger adsorption constant toward V(V).

Under lower loading conditions, elements were first adsorbed onto strong surface sites. Therefore, site $\underline{S}_{2S}$ played the most important role on adsorbing all three elements, as shown in Fig. S1. Under higher loading conditions, the low concentration strong surface site $\underline{S}_{2S}$ were totally saturated. Therefore, high concentration sites such as $\underline{S}_{2W}$ and $\underline{S}_1$ played a more important role in removing sorbates. Figs. S2 and S3 show that site $\underline{S}_{2W}$ became more and more important in adsorbing As(V). In the mean time, site $\underline{S}_{2W}$ was the major site to adsorb Se(IV) under higher loading conditions, and site $\underline{S}_1$ gradually became the major site in adsorbing V(V). Therefore, the relative importance of each surface site on adsorption is significant related to the surface loading and their respective adsorption constants.

5. Conclusions

Predicting the competitive adsorption behavior among toxic anions is important in determining the field capacity of the adsorption media under various water quality conditions. This study investigated the competitive adsorption among As(V), Se(IV), and V(V), and developed a speciation-based competitive adsorption model. This speciation-based model satisfactorily predicted the adsorption of As(V), Se(IV), and V(V) onto activated alumina in multi-sorbate systems over a pH range of 1.5–12, and a wide surface loading range of up to 60 mg/g sorbent, using the same set of adsorption constants generated from single-sorbate systems. The surface loading and the adsorption constant of each element species determine the adsorption behavior of the media for each element. The speciation-based competitive adsorption model is of great significance in predicting the adsorption capacity of activated alumina under various pH and surface loading conditions when other competing elements are present. This model expands the traditional Langmuir isotherm by incorporating the effects of pH and competing sorbates.

Acknowledgement

This research was partially supported by the Environmental Research Center (ERC) at the Missouri University of Science and Technology. Special thanks to Ms. Honglan Shi, Chemist at ERC, for her help in chemical analysis and instrument training. Conclusions and statements made in this paper are those of the authors, and in no way reflect the endorsement of the aforementioned funding party.

Appendix A. Supplementary data

Supplementary data associated with this article can be found, in the online version, at doi:10.1016/j.jhazmat.2009.11.052.

References

[1] C.D. Rail, W.M. Hadley, Selenium in water. An overview, J. Environ. Health 39 (1976) 173–175.
[2] K.G. Brown, G.L. Ross, Arsenic, drinking water, and health: a position paper of the American Council on Science and Health, Regul. Toxicol. Pharmacol. 36 (2002) 162–174.
[3] E. Veschetti, D. Maresca, L. Lucentini, E. Ferretti, G. Citti, M. Ottaviani, Monitoring of V(IV) and V(V) in Etnean drinking-water distribution systems by solid phase extraction and electrothermal atomic absorption spectrometry, Microchem. J. 85 (2007) 80–87.
[4] US EPA, National Primary Drinking Water Regulations: Ground Water Rule, 2003, EPA-HQ-OW-2002-0061, FRL-8046-5.
[5] US EPA, Announcement of the Drinking Water Contaminant Candidate List, 1998, W-97-11, FRL-5972-5.
[6] US EPA, Drinking Water Contaminant Candidate List 2, Final Notice, 2005, OW-2003-0028, FRL-7876-9.
[7] US EPA, Drinking Water Contaminant Candidate List 3—Draft, 2008, EPA-HQ-OW-2007-1189 FRL-8529-7.
[8] OEHHA, CA.GOV, Notification Levels for Chemicals in Drinking Water, http://oehha.ca.gov/water/pals/index.html.
[9] S.A. Davis, M. Misra, Transport model for the adsorption of oxyanions of selenium (IV) and arsenic (V) from water onto lanthanum- and aluminum-based oxides, J. Colloid Interface Sci. 88 (1997) 340–350.
[10] T.F. Lin, J.K. Wu, Adsorption of arsenite and arsenate within activated alumina grains: equilibrium and kinetics, Water Res. 35 (2001) 2049–2057.
[11] T.S. Singh, K.K. Pant, Equilibrium, kinetics and thermodynamic studies for adsorption of As(III) on activated alumina, Sep. Purif. Technol. 36 (2004) 139–147.
[12] T. Su, X. Guan, G. Gu, J. Wang, Adsorption characteristics of As(V), Se(IV), and V(V) onto activated alumina: effects of pH, surface loading, and ionic strength, J. Colloid Interface Sci. 326 (2008) 347–353.
[13] J.P. Gustafsson, Modelling competitive anion adsorption on oxide minerals and an allophane-containing soil, Eur. J. Soil Sci. 52 (2001) 639–653.
[14] A. Jain, R.H. Loeppert, Effect of competing anions on the adsorption of arsenate and arsenite by ferrihydrite, J. Environ. Qual. 29 (2000) 1422–1430.
[15] Y. Jeong, M. Fan, J. Van Leeuwen, J.F. Belczyk, Effect of competing solutes on arsenic(V) adsorption using iron and aluminum oxides, J. Environ. Sci. (Beijing, China) 19 (2007) 910–919.
[16] B.A. Manning, S. Goldberg, Modeling arsenate competitive adsorption on kaolinite, montmorillonite and illite, Clays Clay Miner. 44 (1996) 609–623.
[17] J.A. Wilkie, J.G. Hering, Adsorption of arsenic onto hydrous ferric oxide: effects of adsorbate/adsorbent ratios and co-occurring solutes, Colloids Surf. A 107 (1996) 97–110.
[18] Y. Gao, A. Mucci, Individual and competitive adsorption of phosphate and arsenate on goethite in artificial seawater, Chem. Geol. 199 (2003) 91–109.
[19] H. Zeng, B. Fisher, D.E. Giammar, Individual and competitive adsorption of arsenate and phosphate to a high-surface-area iron oxide-based sorbent, Environ. Sci. Technol. 42 (2008) 147–152.
[20] Y. Gao, A. Mucci, Acid base reactions, phosphate and arsenate complexation, and their competitive adsorption at the surface of goethite in 0.7 M NaCl solution, Geochim. Cosmochim. Acta 65 (2001) 2361–2378.
[21] J.P. Gustafsson, Arsenate adsorption to soils: modelling the competition from humic substances, Geoderma 136 (2006) 320–330.
[22] US EPA, Arsenic Treatment Technologies for Soil, Waste, and Water, 2002, EPA-542-R-02-004, 2-1.
[23] Y.T. Chan, W.H. Kuan, T.Y. Chen, M.K. Wang, Adsorption mechanism of selenate and selenite on the binary oxide systems, Water Res. 43 (2009) 4412–4420.
[24] B. Wehrli, W. Stumm, Vanadyl in natural waters: adsorption and hydrolysis promote oxygenation, Geochim. Cosmochim. Acta 53 (1989) 69–77.
[25] W. Driehaus, M. Jekel, U. Hildebrandt, Granular ferric hydroxide—a new adsorbent for the removal of arsenic from natural water, Aqua (Oxford) 47 (1998) 30–35.
[26] U. Forstner, I. Haase, Geochemical demobilization of metallic pollutants in solid waste—implications for arsenic in waterworks sludges, J. Geochem. Explor. 62 (1998) 29–36.
[27] K.-H. Goh, T.-T. Lim, Geochemistry of inorganic arsenic and selenium in a tropical soil: effect of reaction time, pH, and competitive anions on arsenic and selenium adsorption, Chemosphere 55 (2004) 849–859.